

Hydrodynamic Engineering Approaches for Modeling of the Surface Cell Morphogenesis as Applications of Rosen's Optimality Theory

Alexander S. Bolkhovitinov
IMS, New York, USA
Email: a.s.bolkhovitinov@gmail.com

Abstract—This paper considers the application of Kutta-Joukowski law for description of a number of phenomenon inherent to biological cells in the framework of Rosen biological optimality theory. The applicability of this approach to model artificial cells is demonstrated and the possible application of similarity theory together with dimensional theory for this purpose is also outlined.

Index Terms—kutta-joukowski theorem, optimality theory, cell morphogenesis, hydrodynamics, artificial cells, surface

I. INTRODUCTION

Less than a year ago our Russian colleague in his paper [1] considered the problem of artificial cell deformation from the standpoint of nonlinear dynamics. Earlier he has shown that iCELL deformations, changing their shape and leading to interactions between them, can be induced by external effects [2].

Since the mechanics of such cells is similar to bubble mechanics [3], it is obvious that iCELL nonlinear dynamics is equivalent to nonlinear hydrodynamics of the microbubble medium [4]. As the cell boundaries are also phase boundaries, surface deformations cause surface tension changes on them [5]. It is obvious that surface tension causing bubble deformation during its growth, is due to buoyancy forces [6], i.e. the force gradient at the interface. Such systems can be easily simulated using Joukowski equations because Kutta–Joukowski lift is also caused by a lifting force.

This fact does not imply that the cell itself should possess a lifting force like a wing, as it is inconsistent with experimental observations. Joukowski equation can be applied to other kinds of forces more likely observed in biological systems. For example, its applicability to the calculation of electric fields was shown in [7], which can be used in various electrical concepts of morphogenesis and behavior of living systems (galvanotropism, electromorphology, galvanotaxis, etc). In [8] Joukowski equation was used for isothermal curve calculation and its the calculation of isoenergetic families of orbits was also performed using this equation in [9]. Its universal applicability to the general cases of asymptotic trajectories of dynamical systems [10], resulting in a successful use of this approach in the case of the

structures described in [1], is consistent with the applicability of hydrodynamic equations to electrodynamic and other systems (Laplace equation, etc) [11]. Indeed, as it was correctly stated in [12]: "The combination of problems involving particle dynamics and those involving dynamics of nonlinear media in absence of collisions brought about a sort "physical laboratory," in which it proved possible to demonstrate a real physical analogue of virtually any process from any other domain of physics".

However, if we assume that hydrodynamic lifting force is the cause of mobility and deformability, then Joukowski formula can be applied for gliding (passive) flight modeling in artificial cell analogs found in plankton [13].

The formal phenomenological convergence of cell biophysics and aerohydrodynamics characterized by Joukowski transforms occurs in an unexpected area - the string theory where Joukowski variable is used [14]. Since the strings along with branes - membranes in M-theory are extended objects, it is possible to describe the formation of their analogs such as strings and membranous structures formed in biochemical systems [15]-[17] using Joukowski formula. However, as such systems possess the analogy with cell communication [18-20], it would be useful to relate this approach to cell assembly formation due to their mutual force interactions, described in [1]. A particular interest in Joukowski theory application to biomimetic structures [15]-[17] self-assembly description is due to the fact that those structures in some cases possess chirality [21]-[25], while in the framework of the string theory chiral anomalies are possible [26]-[30] with both the strings and membranes (branes) formed from them [31]-[35] demonstrating a sort of chirality. Certainly, biological chirality is not the same as chirality at cosmological level, but it does not negate the applicability of Joukowski equation to chiral objects at the appropriate organization scale. As far as we know, N. E. Joukowski did not limit the applicability of his formalism for the distant branches of knowledge and matter organization scales [36], which corresponds to the theory of similarity and scale invariance in hydrodynamics [37]. Hence, in this way the applicability of Joukowski formalism to the membrane theory appears to be model in this case with respect to the same property in biophysical chemistry.

Its applicability to capsular cell models like inorganic cells would be an appropriate model of morphogenesis and hydrodynamically induced evolutionary dynamics [38], [39] in biological cells [40], [41] (However, this statement, as well as the book cited illustrating this thesis, is far from certain, but this assumption is not necessary because of the above mentioned applicability of Joukowski equation to the fields of non-hydrodynamic nature). The morphological analogy between the bubbles and protocells is not random. It is due to the unity of the physical principles determining their form [42], osmotic and transport processes in them [43].

In this regard, to date a very little number of works have been published on the specific study of microbiological morphology spontaneous morphogenesis under hydrodynamic forces of the surrounding media except the old papers by A. Bary [44]-[47] which have recently been reprinted by "print on demand". He considered either photophysical [48], or endogenous physiological and biochemical factors [49] as the taxis driving force in microbiological morphogenesis. To our knowledge, de Bary in his work "Vergleichende Morphologie und Biologie der Pilze, Mycetozen und Bacterien", challenging Rozanoff hypothesis on principle of geotropic plasmodium movement and deformation, attached a great importance to cell hydrotropism with rheotropism and thermotropism coupled to it in reaction-diffusion processes of mass transfer (to date most of papers by de Bary still remain relevant and are of great historical interest; for example, see supplementary papers [68]-[70]). Meanwhile, the possibility of morphologically, geometrically and topologically similar microstructure formation [50] during artificial cell synthesis (in particular, inorganic iCHELLs) in the absence of genetic code and complex biochemical machinery makes it necessary to explain their habit formation under the influence of single external physico-chemical factors without biochemical ones. In other words, primitive cellular form morphogenesis and deformation simulation can be performed using hydrodynamic methods, particularly with the Joukowski formalism, and it is possible to apply them to inorganic cells: iCHELLs or their analogs.

Thus we propose to use Kutta-Joukowski theorem & equation and Joukowski transform for artificial cell (iCHELL) morphogenesis and behavior simulation. According to Rosen optimality theory [51] cited in hydrodynamic description of growing forms by Darwin in ecohydrology [52] one can take the most effective flow forms as optimum. Thus, we reduce the calculations to the minimum by rejecting ineffective further eliminated hydrodynamic flow profiles. The subsequent varying of certain parameters and variables provides a number of evolutionary and hydrodynamically optimal morphologies, and then we can visualize the flow around them as iterative optimization for standard morphological and physiological functions realization. This condition can be seen by reference to Kutta-Joukowski theorem and generally known similarity theory.

II. HELPFUL HINTS

The calculation were performed using Joukowski Transform NASA Applet developed by Glenn Research Center or by FoilSimU III (it can be downloaded from <http://www.grc.nasa.gov/WWW/K-12/airplane/foil3u.html>).

For a better understanding of the material given below let us introduce some minimal necessary information about the formalism used. The calculation and visualization was carried out using Joukowski function - a conformal mapping (it is one of the classical elementary functions in complex analysis, as most of trigonometric and hyperbolic functions can be represented as a superposition of exponential function and Joukowski function) which is defined as a complex plane transformation:

$$f : C \setminus \{0\} \rightarrow C \quad (1)$$

by the equation

$$f(z) = \frac{1}{2} \left(z + \frac{1}{z} \right) \quad (2)$$

A similarity can be also written

$$z = \zeta + \frac{1}{\zeta} \quad (3)$$

where $z = x + iy$ and $\zeta = \chi + i\eta$.

The bend angle and the profile thickness can be changed by varying the circle radius and position relative to 0. The circle center coordinates are variable and their different values change the profile shape (here and further the airfoil analog). The circle encloses the point $\zeta = -1$ and crosses the point $\zeta = 1$. This can be achieved for any admissible center position $\mu_x + i\mu_y$, by varying the radius. In general, the transformation of any complex number ζ to z can be realized as:

$$\begin{aligned} z = x + iy &= \zeta + \frac{1}{\zeta} = \\ &= \chi + i\eta + \frac{1}{\chi + i\eta} = \chi + i\eta + \frac{(\chi + i\eta)}{\chi^2 + \eta^2} = \\ &= \frac{\chi(\chi^2 + \eta^2 + 1)}{\chi^2 + \eta^2} + i \frac{\eta(\chi^2 + \eta^2 - 1)}{\chi^2 + \eta^2} \end{aligned} \quad (4)$$

Thus, the real (x) and imaginary (y) components are:

$$x = \frac{\chi(\chi^2 + \eta^2 + 1)}{\chi^2 + \eta^2} \quad (5)$$

$$y = \frac{\eta(\chi^2 + \eta^2 - 1)}{\chi^2 + \eta^2} \quad (6)$$

Joukowski airfoil is usually calculated for a cylinder, but at a low cylinder height it is possible to partly neglect this, calculating the section of an anisometric (or so called prosenchymal) cell in the same way. Then we calculate the complex velocity \tilde{W} on a circle in ζ plane.

$$\tilde{W} = V_\infty e^{-i\alpha} + \frac{iG}{2\pi(\zeta - \mu)} - \frac{V_\infty R^2 e^{i\alpha}}{(\zeta - \mu)^2} \quad (7)$$

where

$\mu = \mu_x + i\mu_y$ - a complex coordinate of a circle centre,

V_∞ - free-stream fluid velocity

α - the angle of attack relative to the oncoming flow,

$$R = \sqrt{(1 - \mu_x)^2 + \mu_y^2} \quad (8)$$

G corresponds to the Kutta condition:

$$G = 4\pi V_\infty R \sin\left(\alpha + \sin^{-1}\left(\frac{\mu_y}{R}\right)\right) \quad (9)$$

The COMPLEX velocity W on the airfoil can be also defined as:

$$W = \frac{\tilde{W}}{\frac{dz}{d\zeta}} = \frac{\tilde{W}}{1 - \frac{1}{\zeta^2}} \quad (10)$$

where

$$W = u_x - iu_y \quad (11)$$

u_x and u_y - the COMPONENT x and y velocity and the directions, respectively, with $z = x + iy$, where both x and y are real.

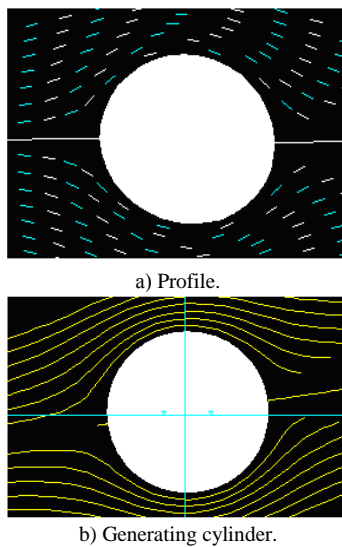


Figure 1. Protoplast profile. Flow parameters (see table):

Radius: 3.486
X-val, Y-val: 0.128
Angle, deg: 8.6
Camber, %: 6.4
Thick, %: 12.975
Circulation: none
No Kutta Condition

Joukowski transform, giving the potential flow for the airfoil corresponding to the given circle, was applied to the result of the potential flow calculation for the circle in

2D case. For the cell it can set the directions of cell movement during morphogenesis under exogenous flows. For the purpose of more precise representation Joukowski function can be considered as superposition of three functions with the corresponding parameter. For example, Karman-Trefftz transformation can be used:

$$f(z) = \frac{1}{2}\left(z + \frac{1}{z}\right) = S_3(S_2(S_1(z))) \quad (12)$$

where

$$S_3(z) = \frac{1+z}{1-z}, \quad (13)$$

$$S_2(z) = z^2, \quad (13)$$

$$S_1(z) = \frac{z-1}{z+1}. \quad (13)$$

III. SIMULATION RESULTS.

A. Cell Deformations in Morphogenesis and Cytotomy

Let us assume that the initial cell has an almost round profile. Then the cell flow profile will have a form shown in Fig. 1a with generating cylinder shown in Fig. 1b. In the case shown the radius was 3.468 y.e., X-val = Y-val = 0.128, the slope angle was 8.6 deg (that is however not important for the cylinder), camber was 6.4 % and thickness was equal to 12.975% without circulation.

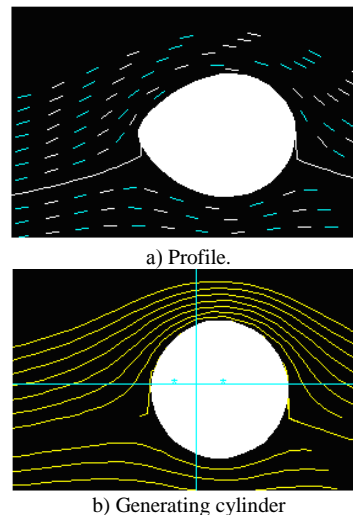


Figure 2. Cell deformation profile. Flow parameters (see table):

Radius: 2.832
X-val: 0.98
Y-val: -0.234
Angle, deg: -2.12
Camber, %: -6.9
Thick, %: 6.85
Circulation: 1.96
No Kutta Condition

Next we begin to deform the cell changing the values of the variables or the parameters. Fig. 2-4 demonstrate cell profiles without Kutta condition (a) and their generative cylinders (b) with the specified sequence of the varied values. In this way one can obtain curved “cells” morphologically similar to the vibrio and abnormal drop-shaped structures obtained earlier by the authors [1] (for example see Fig. 5-6).

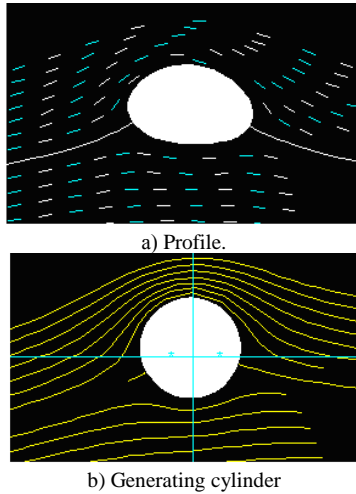


Figure 3. Cell deformation profile. Flow parameters (see table):

Radius: 2.108
X-val: -0.084
Y-val: 0.362
Angle, deg: 5.0
Camber, %: 24.5
Thick, %: 25.75
Circulation: 1.704
No Kutta Condition

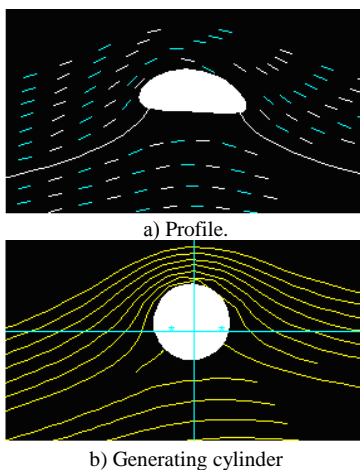


Figure 4. Cell deformation profile. Flow parameters (see table):

Radius: 1.552
X-val: -0.084
Y-val: 0.362
Angle, deg: 5.0
Camber, %: 24.5
Thick, %: 25.75
Circulation: 1.96
No Kutta Condition

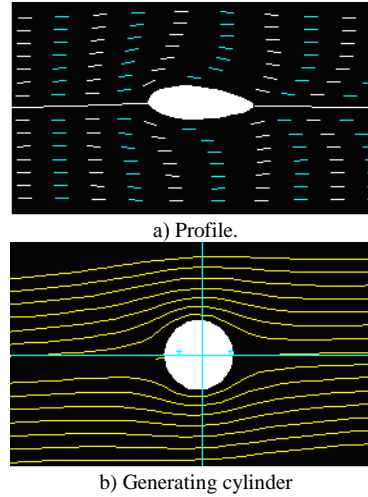


Figure 5. Cell deformation profile. Flow parameters (see table):

Radius: 1.384
X-val: -0.134
Y-val: 0.0
Angle, deg: 3.0
Camber, %: 0.0
Thick, %: 12.5
Circulation: 0.116
No Kutta Condition

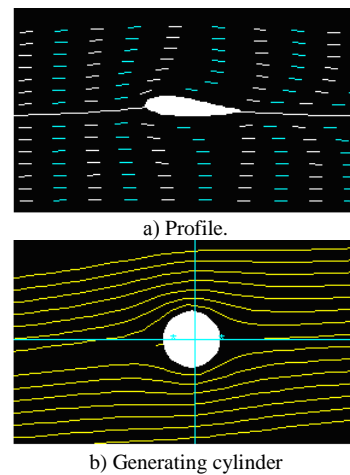
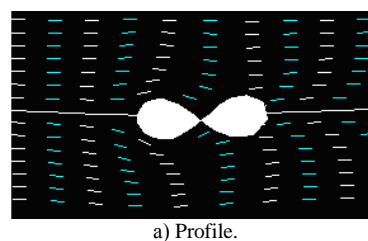
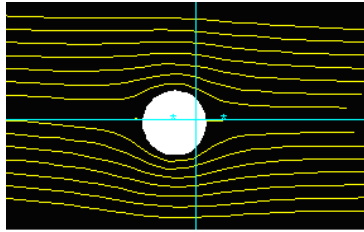


Figure 6. Cell deformation profile. Flow parameters (see table):

Radius: 1.212
X-val: -0.134
Y-val: 0.0
Angle, deg: 5.0
Camber, %: 0.0
Thick, %: 12.5
Circulation: 0.196
No Kutta Condition

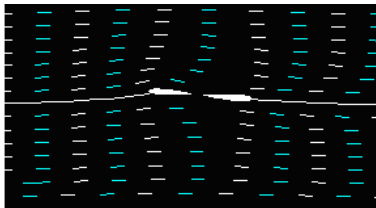




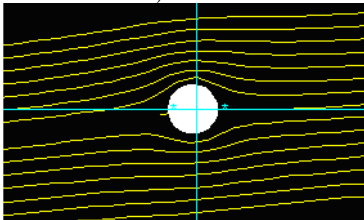
b) Generating cylinder

Figure 7. Cell division profile. Flow parameters (see table):

Radius: 1.296
X-val: -0.83
Y-val: 0.183
Angle, deg: -2.12
Camber, %: -6.9
Thick, %: 27.75
Circulation: -0.212
No Kutta Condition



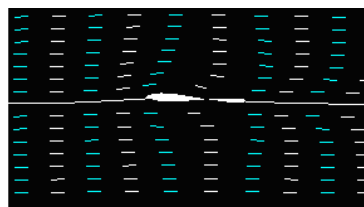
a) Profile.



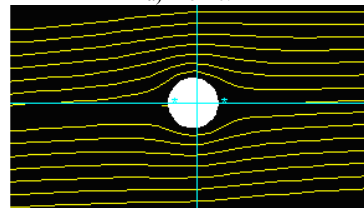
b) Generating cylinder

Figure 8. Cell division profile. Flow parameters (see table):

Radius: 1.0
X-val: -0.134
Y-val: 0.0
Angle, deg: 5.0
Camber, %: 0.0
Thick, %: 12.5
Circulation: 0.196
Kutta Condition



a) Profile.



b) Generating cylinder

Figure 9. Cell division profile. Flow parameters (see table):

Radius: 1.044
X-val: -0.134
Y-val: 0.0
Angle, deg: 3.0
Camber, %: 0.0
Thick, %: 12.5
Circulation: -0.116
Kutta Condition

Cell cytotomy in the flow can be simulated in a similar way in a similar way. Fig. 7-9 show examples of cytotomy simulation using the above approach. Fig. 7 demonstrates the result without Kutta condition and Fig. 8, 9 – with Kutta condition. Comparison of Fig. 8 and Fig. 9 provides the evidence for the possibility of asymmetrical cell division / amitosis (on asymmetric cell division, see for example supplementary literature [71]-[75]) simulation, which is morphologically described in recently reprinted old papers [53] and [54], [55]. This data were comprehensive enough for that stage of the science development and do not contradict to contemporal data [56] in the framework of their recognition within simple models similar to those described in this paper.

The program also provides numerical data on the upper and low surface profile (see Table I & II) and simulation parametric elements. The examples of parametric for two cases of an elliptical profile with and without the curvature are given in Tables III, IV. From the simulation data which do not possess numerical correspondence to biological or biomimetic forms, that follows from the absolute values given in the tables, but are related to them in terms of the similarity theory in its classical mechanical form [57]-[61] (significant results in the area of similarity theory and dimension analysis are described in: Milisavlevich B.M. Dimensional Analysis and Similarity Theory in Applied Mechanics and Heat Transfer, Wiley-ISTE, 2013 (in press) and other works), the flow optimality oscillations can also be obtained for the deformed artificial cells.

TABLE I. THE UPPER SURFACE

X/c	Y/c	P	V
-0.511	0.044	2.079	229
-0.503	0.062	1.771	382
-0.483	0.078	1.694	411
-0.45	0.09	1.716	403
-0.406	0.098	1.756	388
-0.351	0.102	1.799	371
-0.287	0.101	1.839	354
-0.215	0.095	1.878	337
-0.136	0.084	1.913	321
-0.052	0.07	1.946	305
0.033	0.052	1.976	289
0.12	0.033	2.003	275
0.204	0.014	2.027	262
0.283	-0.0030	2.047	250
0.355	-0.019	2.063	240
0.414	-0.03	2.077	231
0.46	-0.038	2.087	224
0.488	-0.042	2.093	220
0.498	-0.043	2.253	0

TABLE II. LOWER SURFACE

X/c	Y/c	P	V
-0.511	0.044	2.079	229
-0.507	0.025	2.253	0
-0.489	0.0070	2.19	138
-0.459	-0.01	2.115	205
-0.417	-0.026	2.067	237
-0.364	-0.04	2.041	254
-0.3	-0.05	2.029	261
-0.228	-0.056	2.026	262
-0.149	-0.06	2.03	260
-0.064	-0.06	2.037	256
0.023	-0.057	2.047	250
0.112	-0.053	2.058	243
0.199	-0.049	2.068	237
0.28	-0.045	2.078	230
0.353	-0.042	2.086	225
0.413	-0.041	2.092	220
0.459	-0.041	2.097	218
0.488	-0.042	2.098	216
0.498	-0.043	2.253	0

TABLE III. A PROFILE WITH A CURVATURE.

Elliptical Profile
Camber = 19.6 % chord ,
Thickness = 19.791 % chord ,
Chord = 5.0 ft ,
Span = 20.0 ft ,
Surface Area = 100.0 sq ft ,
Angle of attack = 0.0 degrees ,
Standard Earth Atmosphere
Altitude = 45800 ft ,
Density = 4.4E-4slug/cu ft
Pressure = 2.051lb/sq in,
Temperature = -70F,
Airspeed = 247 mph ,
Lift = 5877 lbs
Drag = 1467 lbs

TABLE IV. A PROFILE WITHOUT A CURVATURE .

Elliptical Profile
Camber = 0.0 % chord,
Thickness = 19.81 % chord,
Chord = 5.0 ft ,
Span = 20.0 ft ,
Surface Area = 100.0 sq ft ,
Angle of attack = 0.0 degrees ,
Standard Earth Atmosphere
Altitude = 45800 ft ,
Density = 4.4E-4slug/cu ft
Pressure = 2.051lb/sq in,
Temperature = -70F,
Airspeed = 247 mph ,
Lift = 0.0 lbs
Drag = 109 lbs

Table II is correct for the following parameter values: camber = 0.0 % chord, thickness = 12.5 % chord, chord = 5.0 ft, span = 20.0 ft, angle of attack = 5.0 degrees, SEA (Standard Earth Atmosphere), ambient pressure = 2.051lb/sq in, ambient velocity = 247 mph. But this may seem rather pointless in light of the Buckingham (Vaschy - Buckingham) π theorem or nondimensionalization using Rayleigh's method of dimensional analysis.

For many purposes, this approach is useful as it stands and this is made plausible by intuitive-logical arguments. It is easy to see that this condition is necessary. But let us return to the general idea of this paper.

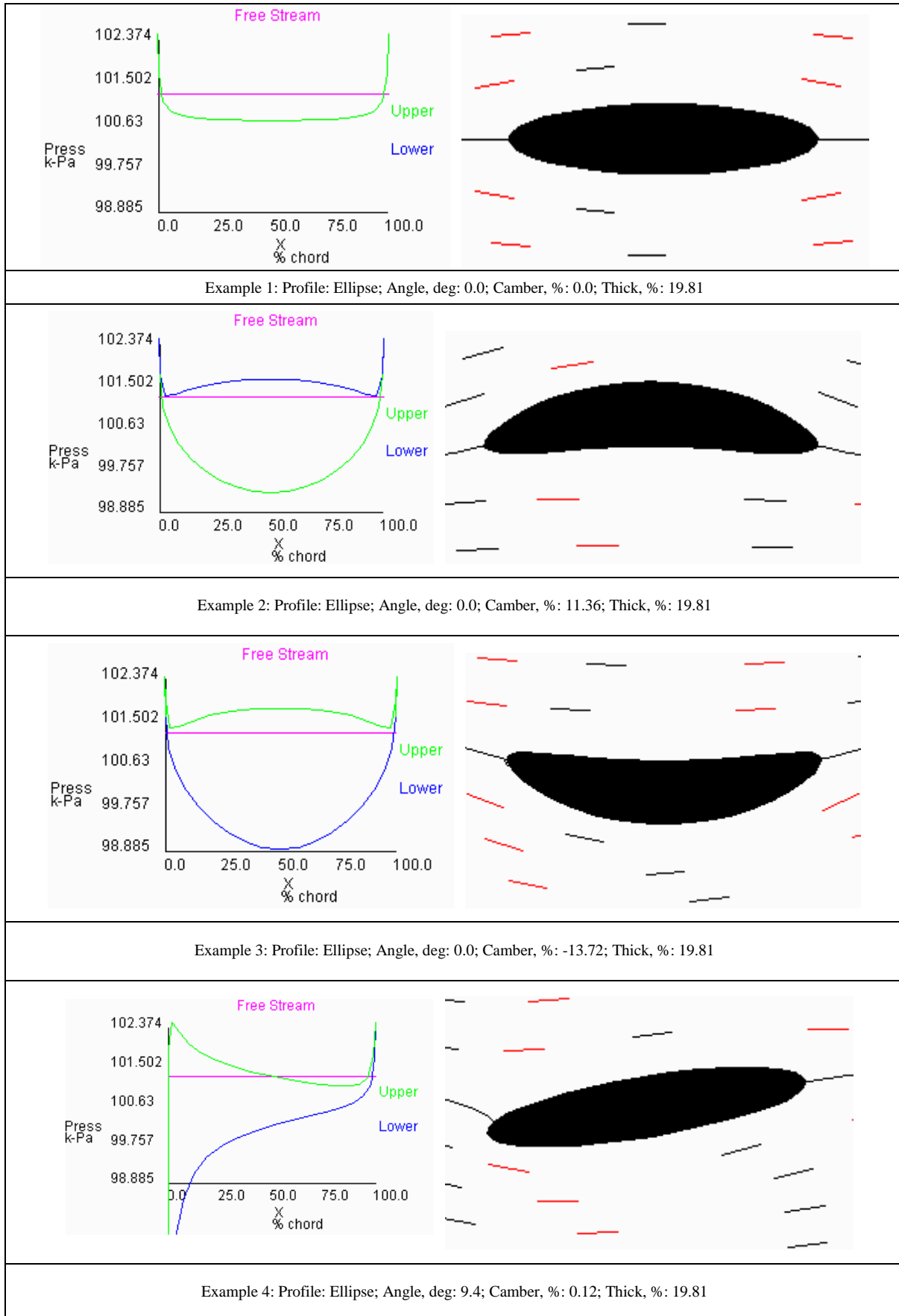
We can demonstrate the above statement by examining the changes in the dependence of hydrodynamic efficiency on the cell deforming pressure. The numerical simulation data are given in the Table V. The initial unperturbed cell habit (Example 1) shows a symmetrical response to pressure regardless of its direction (Examples 2, 3) but changes the curve character during active angular motion in the flow (Example 4). In the case of a simultaneous change in the attack angle and the profile curvature (Examples 5, 6) these relationships change asymmetrically also regardless of the attack direction changes (compare Example 5 with Example 7; Example 4 with Example 8).

B. Concept verification using model iCHELLs.

As follows from the above material, bacillus-like cells can be described as wing airfoils and can be easily transformed into vibrio-like forms. Similar results can be observed with iCHELLs – cell differentiation models. If the above assumptions are correct, generation cylinder corresponding to a round iCHELL or a similar structure should take a curved shape under deformations and long-term optimality selection in a hydrodynamic medium. This effect is really observed in the experiments. We asked the author of [1, 2] to provide artificial cell images with serious deformations. The micrographs given below indicate the presence of significant perturbations of hydrodynamic or some other nature during artificial cell morphology formation or development. Fig. 10 demonstrates the cell deformation (distortion, curvature) with the curvature of the “cytoskeleton” (or at least its central “axis”), which is consistent with biomechanical principles. Small cells have little or no deformations suggesting that deformation occurs only with the critical surface area required for the development of the cell lifting “force”. Examples of such curvatures are given in Table V

The dependence of bending degree on the critical surface area and cell length and width proportions can be demonstrated in another example. Artificial cells obtained in another chemical medium are shown in Fig. 11. The smallest cell is only slightly deformed while the two long cells are strongly curved and tend to asymmetric cell division as predicted by Fig. 7-9. This division possesses a remarkable feature from the standpoint of mechanics: the total surface area after it becomes reduced and as a result hydrodynamic properties of the division products change significantly. This statement can be proved by the thickness changing of the boundary layer flowing over the cell division products (see Fig. 12). The changes observed can be illustrated using simulation data outlined in the theoretical section of this article by plotting the lifting force (which is the correlate of specific surface area) dependence on the other variables for an abstract profile. The results are given in Table VI

TABLE V. GRAPHICAL EXAMPLES THE DEPENDENCE OF HYDRODYNAMIC EFFICIENCY ON THE CELL DEFORMING PRESSURE.



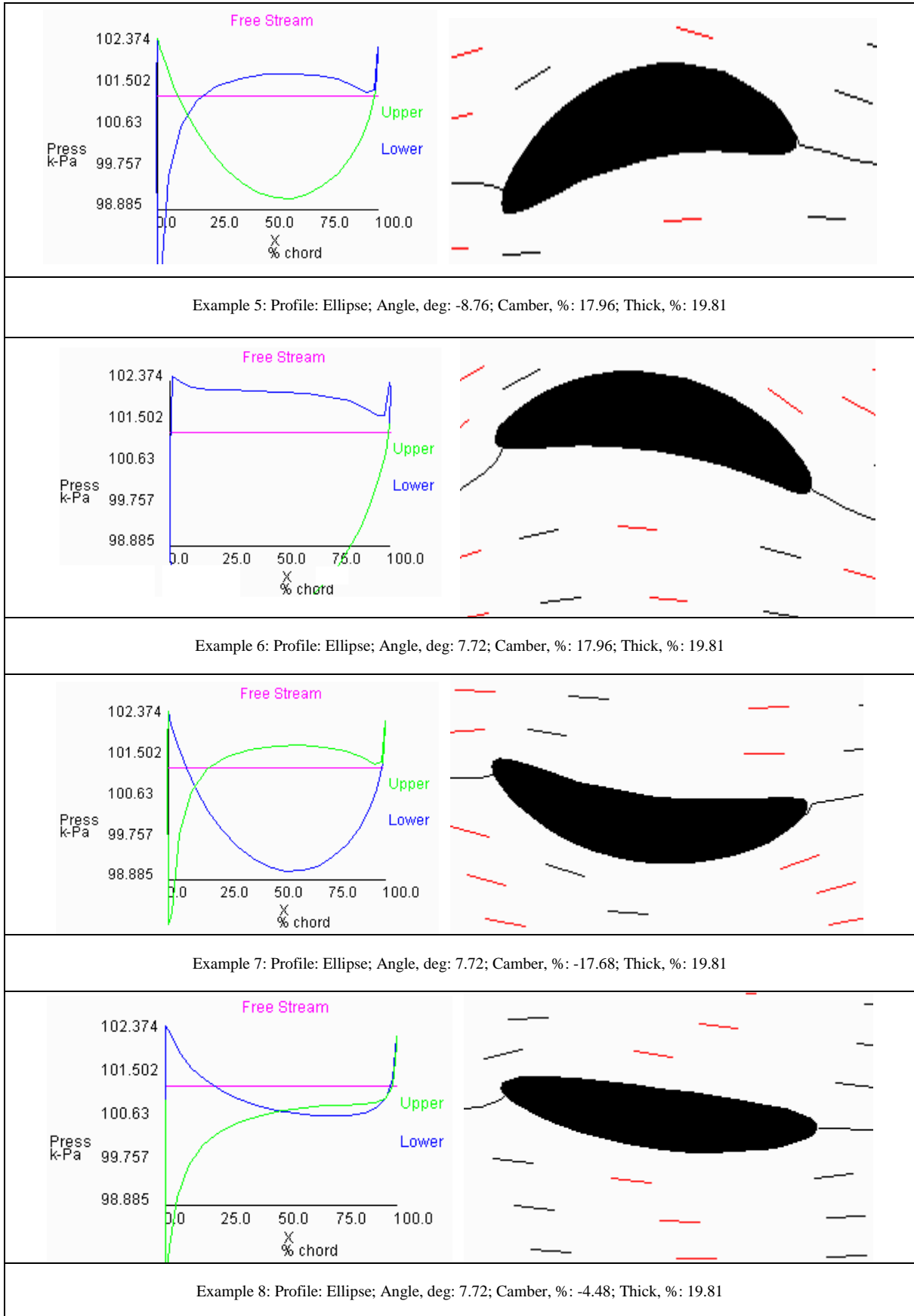


TABLE VI. PLOTTING THE LIFTING FORCE CURVES (WHICH IS THE CORRELATE OF SPECIFIC SURFACE AREA)

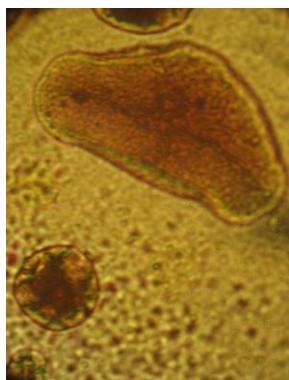
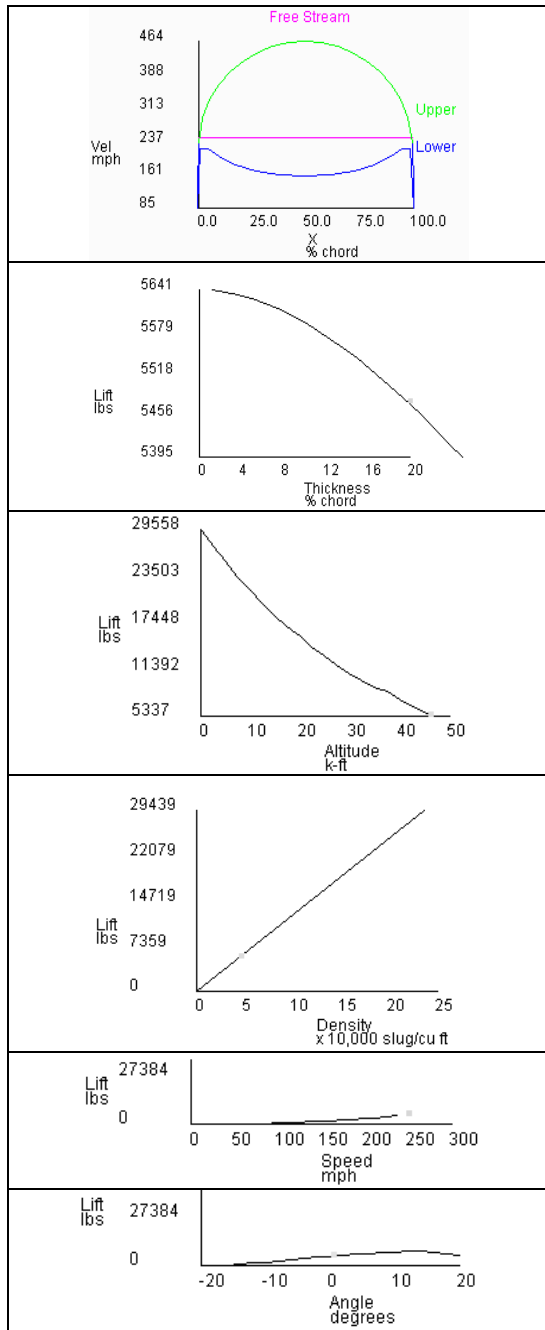


Figure 10. An example of artificial cell bending with the "cytoskeleton" curvature change

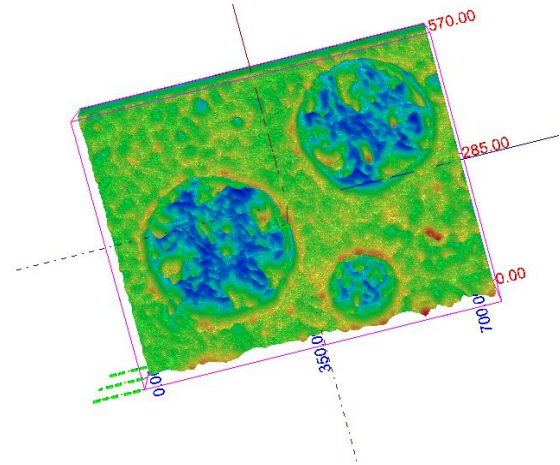


Figure 11. Artificial cells with different specific surface area

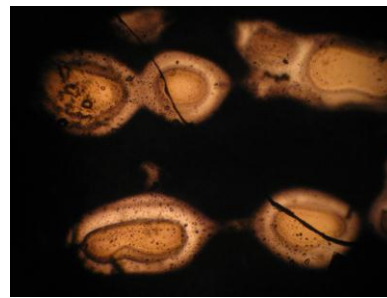


Figure 12. An example of artificial cell bending with the "cytoskeleton" curvature change

Let us define the above findings mathematically. The length to width ratio (i.e. parenchymal or prosenchymal cell type) for a model cell profile is a correlate of 'aerodynamic characteristics' - lift-drag ratio in the flow coordinate system with the given attack angle (cell increment / decrement in the medium):

$$K(\alpha) = \frac{C_{ya}(\alpha)}{C_{xa}(\alpha)}$$

where

α — the attack angle;

C_{xa} — drag coefficient;

C_{ya} — lift parameter.

Since the total aerodynamic force is integral of the pressure about a closed path:

$$Y + P = \oint_{\partial\Omega} p n d\Omega$$

where:

Y — lifting force,

P — thrust,

$\partial\Omega$ — airfoil boundary,

p — pressure,

n — normal to the airfoil,

the corresponding total force for the cell will be determined by the osmotic pressure around its contour. At the same time the resistance scalar value is proportional to the characteristic area S . The latter for spherical cells is cross-section area, for rotating flagella - the area of "blades," for prosenchymal cells oriented along the flow -

the volumetric area, and for cilia rows - their envelop surface area. Since the cell movement in the surrounding medium is rather slow, it is possible to use the induced drag to explain the effects observed in terms of the optimality theory. The induced drag is proportional to the square of the lifting force Y and is inversely proportional to the bearing surface S , its elongation λ , the medium density ρ and the square of speed V . This makes apparent the reasons for size heterogeneity (together with length to width ratio and dynamic characteristic heterogeneity) emergence in the populations of moving artificial cells observed in Fig. 13 at low magnification.

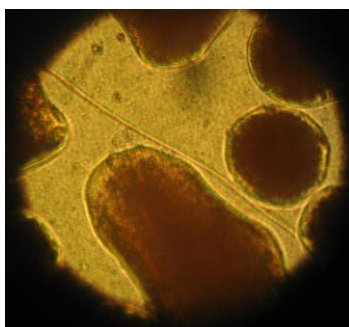


Figure. 13. iCHELL population heterogeneous in size and aerodynamic parameters

IV. DISCUSSION

From the standpoint of possible dimensional unification in the framework of group theory [62] and differential equation optimality [63] it is possible for the model simulating the prototype shape (form) to simulate the prototype group theoretic properties described by differential equations. If the iCHELL is a cell model and a certain airfoil is an iCHELL model in terms of Kutta-Joukowski theorem, then (if cell division and shape changing can be simulated using iCHELLs), Kutta-Joukowski law simulation for the corresponding iCHELL profile forms (or their airfoils) can reveal the parameter optimality areas for a similar type morphogenesis of biological cells. Since the optimality theory is widely used not only in aerodynamics [64], but also in electrophysics [65], it is possible to simulate electric field distribution in cell model electrophysiology with the computer calculation of similarity relations [66]. The only difference between the standard experimental similarity measurements using wind tunnels and similar equipment [67] and the recent approach proposed lies in the application of simulation modeling and the comparison of the results obtained with the secondary cell model - iCHELL instead of living cells. In subsequent studies we expect to apply the above approach in comparison with native biological cells.

ACKNOWLEDGMENT

The author is grateful to Olle Gradoff for providing artificial cell micrographs and to his colleagues from Moscow State University for recommended biological literature and useful consultations in the biological area.

REFERENCES

- [1] O. Gradoff, "Nonlinear dynamical systems as models of development of inorganic cells (iCHELLs) & their Simple assemblies," *American Journal of Bioinformatics Research*, vol. 2, no. 5, pp. 92-101, 2012.
- [2] O. Gradoff, "Visualization of photoinduced self-organization processes in reaction-diffusion media for modelling of abiogenesis & primitive waves in morphogenesis," *International Journal of Biophysics*, vol. 2, no. 3, pp. 26-39, 2012.
- [3] S. P. Wrenn, S. M. Dicker, E. F. Small, N. R. Dan, *et al.*, "Bursting bubbles and bilayers," *Theranostics*, vol. 2, no. 12, pp. 1140-1159, 2012.
- [4] S. Velickov, *Nonlinear Dynamics and Chaos with Applications to Hydrodynamics and Hydrological Modelling*, Taylor & Francis, 2004, pp. 336.
- [5] H. Wang, Z.-Y. Zhang, Y.-M. Yang, Y. Hu, and H.-S. Zhang, "Numerical investigation of the deformation mechanism of a bubble or a drop rising or falling in another fluid," *Ch. Phys. B.*, vol. 17, no. 10, pp. 3847-3855, 2008.
- [6] H. Wang, Z.-Y. Zhang, Y.-M. Yang, and H.-S. Zhang, "Surface tension effects on the behaviour of a rising bubble driven by buoyancy force," *Ch. Phys. B.*, vol. 19, no. 2, pp. 026801-1 - 026801-9, 2010.
- [7] L. E. Shchebelina, "Generalization of the Zhukovsky function to the electric field of gratings formed by tilted metallic strips," *Tech. Phys.*, vol. 54, no. 4, pp. 452-456, 2009.
- [8] F. Puel, "Potentials having two orthogonal families of curves as trajectories," *Celest. Mech. and Dynam. Astronom.*, vol. 74, no. 3, pp. 199-210, 1999.
- [9] F. Puel, "Separable and partially separable systems in the light of the inverse problem of dynamics," *Celest. Mech. and Dynam. Astronom.*, vol. 63, no. 1, pp. 41-57, 1995.
- [10] O. V. Druzhinina and A. A. Shestakov, "On limiting properties of Lyapunov asymptotically stable and Zhukovsky asymptotically rigid trajectories of a dynamic system," *Dok. Phys.*, vol. 51, no. 7, pp. 369-370, 2006.
- [11] G. A. Tokaty, *A History and Philosophy of Fluid Mechanics*, Dover Publ., 1994, pp. 272.
- [12] R. Z. Sagdeev, D. A. Usikov, and G. M. Zaslavsky, *Nonlinear Physics*, Harwood Academic Publishers, 1992, pp. 690.
- [13] A. V. Vakhova, "On applicability limits of Zhukovsky's model for gliding flight," *Journ. Math. Sci.*, vol. 146, no. 3, pp. 5811-5819, 2007.
- [14] O. Marchal, "One-cut solution of the β ensembles in the Zhukovsky variable," *Journ. Stat. Mech.*, vol. 2012, no. 1, 2012.
- [15] S. V. Stovbun, A. M. Zanin, A. A. Skoblin, A. I. Mikhailov, and A. A. Berlin, "Phenomenological description of the spontaneous formation of macroscopic strings in low-concentration chiral solutions and the formation of anisometric gels," *Dok. Phys. Chem.*, vol. 442, no. 2, pp. 36-39, 2012.
- [16] S. V. Stovbun and A. A. Skoblin, "Strings, anisometric gels, and solutions in chemical and biological systems," *MUP Bull.*, vol. 67, no. 4, pp. 317-330, 2012.
- [17] S. V. Stovbun, A. M. Zanin, A. A. Skoblin, A. I. Mikhailov, *et al.*, "Macroscopic chirality of strings," *RJP Chem. B.*, vol. 5, no. 6, pp. 1019-1022, 2011.
- [18] S.V. Stovbun and A. A. Skoblin, "Physicochemical simulation of cell-cell commutation," *Bull. Exp. Biol. & Med.*, vol. 152, no. 5, pp. 571-574, 2011.
- [19] S. V. Stovbun, A. I. Mikhailov, A. A. Skoblin, E. E. Bragina, and M. A. Gomberg, "On the supramolecular mechanism of cell-cell commutation," *RJP Chem. B.*, vol. 6, no. 1, pp. 60-64, 2012.
- [20] S. V. Stovbun, "Chirality and homochirality of lipids is necessary to form ld-supramolecular structures of cell-cell communications," *Bull. Exp. Biol. & Med.*, vol. 152, no. 1, pp. 50-52, 2011.
- [21] S. V. Stovbun and A. A. Skoblin, "Molecular and supramolecular structures in biological fluids and their homochiral models," *MUP Bull.*, vol. 67, no. 3, pp. 274-277, 2012.
- [22] S. V. Stovbun, "Formation of wirelike structures in dilute solution of chiral compounds," *RJP Chem. B.*, vol. 5, no. 4, pp. 546-553, 2011.
- [23] S. V. Stovbun, A. A. Skoblin, and V. A. Tverdislov, "Biological fluids as chiral anisometric media," *Bull. Exp. Biol. & Med.*, vol. 152, no. 6, pp. 703-706, 2011.

- [24] S. V. Stovbun, O. N. Krutius, A. M. Zanin, D. S. Skorobogatk, and R. G. Kostyanovskii, "Experimental observation of anisometric structures in solutions with a low gelator content," *RJP Chem. B.*, vol. 5, no. 5, pp. 846-849, 2011.
- [25] S. V. Stovbun and A. A. Skoblin, "Chirotopical phenomena in biological fluids and their homochiral models," *MUP Bull.*, vol. 67, no. 3, pp. 278-281, 2012.
- [26] A. N. Schellekens, "Chiral anomalies in strings theory," *Acta Physica Polonica B.*, vol. 20, no. 4, pp. 287-294, 1989.
- [27] A. N. Schellekens, *Chiral Anomalies in Strings Theory*, Ref. CERN - TH.5193/88, 1988, pp. 10.
- [28] R. D. McArthur, "Wick rotation and infinities in the superstring chiral-anomaly graph," *Phys. Rev. D.*, vol. 41, no. 4, pp. 1193-1204, 1990.
- [29] A. Hatzinikitas, K. Schalm, and P. Van Nieuwenhuizen, "Trace and chiral anomalies in string and ordinary field theory from Feynman diagrams for non-linear sigma models," *Nuclear Physics B*, vol. 518, no. 1-2, pp. 424-454, 1998.
- [30] M. R. Douglas and C. Zhou, "Chirality change in string theory," *Journ. High Ener. Phys.*, Art. No.-014, no. 6, pp. 43, 2004.
- [31] J. Lykken, E. Poppitz, and S. P. Trivedi, "Chiral Gauge Theories from D-Branes," *Phys. Lett. B*, vol. 416, no. 3-4, pp. 286-294, 1998.
- [32] A. Butti, D. Forcella, A. Hanany, D. Vegh, and A. Zaffaroni, "Counting chiral operators in quiver gauge theories," *Journ. High Ener. Phys.*, vol. 11, no. 092, pp. 64, 2007.
- [33] J. Lykken, E. Poppitz, and S. P. Trivedi, "More on chiral gauge theories from D-branes," *Nuclear Physics B.*, vol. 520, no 1-2, pp. 51-74, 1998.
- [34] G. Aldazabal, S. Franco, L. E. Ibanez, R. Rabadan, and A. M. Uranga, "D = 4 chiral string compactifications from intersecting branes," *Journ. Math. Phys.*, vol. 42, no 7, pp. 3103-1 - 3103-24, pp. 24, 2001.
- [35] E. V. Gorbar, V. P. Gusynin, and V. A. Miransky, "Dynamical chiral symmetry breaking on a brane in reduced QED," *Phys. Rev. D*, vol. 64, no 10, pp. 105028-1 - 105028-16, 2001.
- [36] S. Strizhevsky, *Nikolai Zhukovsky: Founder of Aeronautics*, University Press of the Pacific, 2003.
- [37] A. Lesne and M. Lagues, *Scale Invariance: From Phase Transitions to Turbulence*, Springer, 2012, pp. 410.
- [38] T. Schwenk, *Sensitive Chaos: The Creation of Flowing Forms in Water and Air*, RSP, 1996, pp. 232.
- [39] T. Schwenk, *Das Sensible Chaos. Strömendes Formenschaften in Wasser und Luft*, Freies Geistesleben, 2010, pp. 144.
- [40] C. Pozridkis, *Modeling and Simulation of Capsules and Biological Cells*, Chapman and Hall/CRC, 2003, pp. 344.
- [41] C. Pozridkis, *Computational Hydrodynamics of Capsules and Biological Cells*, CRC Press, 2010, pp. 327.
- [42] F. T. Lewis, "The Analogous Shapes of Cells and Bubbles," in *Proc. AAAS*, vol. 77, no. 5, 1949, pp. 149-186.
- [43] D. DeKee, *Transport Processes in Bubbles, Drops and Particles*, CRC Press, 2001, pp. 352.
- [44] A. Bary, *Vergleichende Morphologie Und Biologie Der Pilze, Mycetozen, Und Bacterien*, NABU Press, 2010, pp. 584.
- [45] A. Bary, *Beiträge Zur Morphologie Und Physiologie Der Pilze*, NABU Press, 2011, vol. 1-3, pp. 554.
- [46] A. Bary, *Morphologie Und Physiologie Der Pilze, Flechten Und Myxomyceten*, ULAN Press, 2012, pp. 342.
- [47] A. Bary, *Comparative Morphology and Biology of the Fungi Mycetozoa and Bacteria*, Forgotten Books, 2012, pp. 552.
- [48] *Photomorphogenesis in Plants and Bacteria: Function and Signal Transduction Mechanisms*, Ed. by E. Schäfer and F. Nagy, Springer, 2006, pp. 712.
- [49] F. Mayer, *Cytology and Morphogenesis of Bacteria*, Lubrecht & Cramer Ltd., 1986, pp. 220.
- [50] E. A. Lazar, J. K. Mason, R. D. Macpherson, and D. J. Srolovitz, "Complete topology of cells, grains, and bubbles in three-dimensional microstructures," *Phys Rev. Lett.*, vol. 109, no 9, pp. 095505-1 - 095505-5, 2012.
- [51] Rosen R. Optimality principles in biology, Plenum Press, 1967, pp. 204.
- [52] P. S. Eagleson, *Ecology: Darwinian Expression of Vegetation Form and Function*, Cambridge University Press, 2002, pp. 484.
- [53] H. C. Ross and J. W. Cropper, *Induced Cell-reproduction and Cancer; The Isolation of the Chemical Causes of Normal and of Augmented, Asymmetrical Human Cell-division*, Forgotten Books, 2012, pp. 456.
- [54] W. S. Marshall, *Amitosis in the Malpighian Tubules of the Walking-Stick: Diaperomera Femorata*, Kessinger Pub. LLC, 2010, pp. 12.
- [55] W. Nakahara, *Studies of amitosis: Its Physiological Relations in the Adipose Cells of Insects, and its Probable Significance*, University of Michigan Library, 1918, pp. 48.
- [56] *Asymmetric Cell Division*, Ed. by A. Maciero-Coehlo, Springer, 2010, pp. 260.
- [57] L. I. Sedov, *Similarity and Dimensional Methods in Mechanics*, Taylor & Francis - CRC Press, 1993, pp. 496.
- [58] W. E. Baker, P. S. Westine, and F. T. Dodge, *Similarity Methods in Engineering Dynamics: Theory and Practice of Scale Modeling*, Spartan Books / Hayden Book., 1973, pp. 396.
- [59] A. A. Gukhman, *Introduction to the Theory of Similarity*, Acad. Press, 1965, pp. 256.
- [60] L. I. Sedov, *Design of Models, Dimensions, and Similarity*, Defense Technical Information Center (Foreign Technology D. Wright-Patterson AFB), Ohio, 1964, pp. 25.
- [61] R. A. Gaggioli, *Similarity Analyses of Compressible Boundary Layer Flows via Group Theory*, MRC technical summary report, Mathematics Research Center, United States Army, University of Wisconsin, 1968, pp. 18.
- [62] M. J. Moran, *A Unification of Dimensional and Similarity Analysis via Group Theory*, University of Wisconsin-Madison, 1967, pp. 504.
- [63] G. W. Bluman and J. D. Cole, *Similarity Methods for Differential Equations*, Springer, 1974, pp. 348.
- [64] D. Nixon, *Design of Transonic Airfoil Sections using a Similarity Theory*, NASA, 1978, pp. 21.
- [65] V. A. Venikov, *Theory of Similarity and Simulation: with Applications to Problems in Electrical Power Engineering*, Macdonald & Co., 1969, pp. 494.
- [66] J. C. Farrenkopf, *Similarity Theory Relationships Computerized*, University of Wisconsin-Madison, 1992, pp. 112.
- [67] A. Golovin and V. Tarabarin, *Russian Models from the Mechanisms Collection of Bauman University* (History of Mechanism and Machine Science), Springer, 2010, pp. 252.
- [68] G. Drews, "The developmental biology of fungi - a new concept introduced by anton de bary," *Adv. Appl. Microbiol.*, vol. 48, pp. 213-227, 2001.
- [69] T. Hoppe and U. Kutschera, "In the shadow of darwin: Anton de bary's origin of myxomycetology and a molecular phylogeny of the plasmodial slime molds," *Theory Biosci.*, vol. 129, no 1, pp. 15-23, 2010.
- [70] C. Matta, "Spontaneous generation and disease causation: Anton de bary's experiments with phytophthora infestans and late blight of potato," *Journ. Hist. Biol.*, vol. 43, no. 3, pp. 459-491, 2010.
- [71] A. Faubert, J. Lessard, and G. Sauvageau, "Are genetic determinants of asymmetric stem cell division active in hematopoietic stem cells?" *Oncogene*, vol. 23, pp. 7247-7255, 2004.
- [72] K. Gallagher and L. G. Smith, "Asymmetric cell division and cell fate in plants," *Curr. Opin. Cell Biol.*, vol. 9, pp. 842-848, 1996.
- [73] H. R. Horvitz and I. Herskowitz, "Mechanisms of asymmetric cell division: Two bs or not two bs, that is the question," *Cell.*, vol. 68, pp. 237-255, 1992.
- [74] J. P. Seery and F. M. Watt, "Asymmetric stem-cell divisions define the architecture of human oesophageal epithelium," *Curr. Biol.*, vol. 10, pp. 1447-1450, 2000
- [75] E. B. Abrash and D. C. Bergmann, "Asymmetric cell divisions: a view from plant development," *Dev. Cell*, vol. 16, pp. 783-796, 2009.

Alexander S. Bolkhovitinov

Member of APS & Institute of Mathematical Statistics.